The Society for engineering in agricultural, food, and biological systems

An ASAE Meeting Presentation

Paper Number: 053127

Differentiation of Fungi Using Hyperspectral Imagery for Food Inspection

Haibo Yao, Zuzana Hruska, Kevin DiCrispino, Kori Brabham, David Lewis, Jim Beach

Institute for Technology Development
Building 1103, Suite 118, Stennis Space Center, MS 39529

Robert L. Brown, Thomas E. Cleveland

SRRC, ARS, USDA
1100 Robert E. Lee Boulevard, New Orleans, LA 70124

Written for presentation at the
2005 ASAE Annual International Meeting
Sponsored by ASAE
Tampa Convention Center
Tampa, Florida
17 - 20 July 2005

Abstract. *This paper is part of a project of using hyperspectral imagery to detect pathogens such as mycotoxin-producing fungi, in grain products, such as corn. Traditionally, corn kernels have been examined for evidence of bright greenish-yellow fluorescence (BGYF), indicative of the presence of A. flavus, when illuminated with a high-intensity ultra-violet light. The BGYF approach is time and labor intensive and somewhat inaccurate. Several previous studies have examined spectral-based, non-destructive methods for the detection of fungi and toxins. This research focuses on using spectral image data for fungi and toxin detection. A tabletop hyperspectral imaging system, VNIR-100E, is used in the study for high spectral and high spatial resolution spectral data acquisition. In this paper, a total of five toxin producing fungal species were used in two experiments. They are Penicillium chrysogenum, Fusarium moniliforme, Aspergillus parasiticus, Trichoderma viride, and Aspergillus flavus. All fungal isolates were cultured on agar in Petri-dishes under lab conditions and were imaged on day 5 of growth. The objective of this study is to use hyperspectral imagery for classification of different fungi.*

Keywords: hyperspectral image, fungi, classification.

Introduction

Fungi grow almost everywhere and under most conditions. Some fungi are toxin producing and pose a threat to humans and animals. Thus, it is important to detect and identify different toxin-producing molds. One benefit derived from fungal identification procedures is, knowing which specific toxin is present in a given sample. Once a fungus is identified, it is possible to extrapolate the specific toxins that may be present as a consequence. For example, the presence of *Aspergillus flavus* (*A. flavus*) does not necessarily indicate harmful levels of aflatoxin (toxin produced by *aspergillus spp.*), however, it does mean that the potential for aflatoxin production is present. Another example is that some fungi such as *Aspergillus niger* and *Trichoderma viride* can inhibit the growth of *A. flavus* and subsequent aflatoxin detection (Aziz and Shahin, 1997). Thus, correct identification of a fungus can be helpful in isolating the presence of specific toxins associated with the identified organism. Furthermore, knowing which fungi exist in particular samples helps direct the future focus of detection technology. Applications of fungal detection/identification can be for food inspection, homeland security, household inspection, environmental protection, etc.

Aflatoxin is a toxic metabolic by-product of certain fungi one of which is *A. flavus.* Aflatoxin contaminated corn is dangerous for domestic animals when used as feed and is associated with liver cancer in human beings. Aflatoxin levels in food and feed are regulated by the Food and Drug Administration (FDA). Therefore, the ability to detect *A. flavus* and its toxic metabolite, aflatoxin, is important to the grain industry, especially in corn production.

Thin-layer chromatography and HPLC can be used to quantify aflatoxins present in samples (Brown et al., 2001; Dutta and Das, 2001). Aflatoxin fluorescence response is used for qualitative identification of aflatoxin-producing fungi (Malone et al., 2000; Zeringue et al., 1999). New methods developed in recent years include DNA-based analytical methods (e.g. PCR - Polymerase Chain Reaction) for detection of fungi (Zachova et al., 2004) and enzyme-linked immunoassay for aflatoxin detection (Dutta and Das, 2001).

Research also focused on the development of quick and non-invasive ways for fungal identification. An early study (Birth and Johnson, 1970) based on optical measurements, used fluorescence data for fungal detection on corn. The study found that the ratio between two measurements of the fluoresced energy (at 442 and 607 nm) gave the best results. Aja-Nwachukwu and Emejuaiwe (1994) mentioned colony morphology and color microscopy, and biochemical tests for taxa identification. Greene et al. (1992) and Gordon et al. (1997, 1998, 1999) used FTIR (Fourier Transform Infrared) spectroscopy for *A. flavus* detection on corn. The study looked at differences in spectral features of fungi and different corn backgrounds. Although the process was non-destructive the instrumentation involved may be expensive and the procedure time-consuming.

Yabe et al. (1987) suggested using UV photography for screening of fungi. In his approach, UV light source with 365 nm wavelength was used to irradiate samples of different *Aspergilli*. Images were taken using a UV lens. The result showed that aflatoxin-producing fungi such as *A. flavus* and *A. parasiticus* had gray or black colonies, while the aflatoxin-nonproducing taxa such as *A. oryzae* appeared as white colonies.

Rather than identifying fungi directly, some studies used the existence of a certain toxin as an indicator of the presence of a specific fungus. For example, the detection of aflatoxin means the occurrence of some strains of aflatoxin-producing *Aspergillus*. Fente et al. (2001) used an additive for aflatoxin-producing aspergillus detection. The additive, cyclodextrin, could enhance the natural fluorescence of aflatoxin.

Traditionally, hyperspectral imagery was used for earth remote sensing applications using aerial or satellite image data. Most recently, low cost portable hyperspectral sensing system began available for lab based research like the hyperspectral sensor suite developed by the Institute for Technology Development (http://www.iftd.org). Many studies used hyperspectral imagery for food inspection, such as detection of apple bruise (Lu et al., 2003), fecal contamination on chicken carcass (Lawrence et al., 2001), skin tumor on chicken carcass (Kim et al., 2004), and corn genotype identification (Yao et al., 2004).

The objective of this paper is to develop a quick, simple, non-invasive way for identification of fungi using hyperspectral images. This study used visible-near-infrared hyperspectral images taken by a push-broom hyperspectral imager to identify different toxin-producing fungal isolates. It is assumed that the specific spectral signatures should provide enough information for discriminating between different fungi, including different traits within a single genus.

Instrumentation

The sensor used in this experiment was the VNIR 100E hyperspectral imaging system (Figure 1) developed by the Institute for Technology Development. The VNIR 100E incorporates a patented line scanning technique (U.S. Patent No. 6,166,373) that requires no relative movement between the target and the sensor. The system had the same configuration as in Yao et al. (2004). The resulting image was approximately 12.2 × 9.3 cm in area, with pixel resolutions of 0.171 (h) × 0.177 (v) mm^2. The spectral range was from 450 nm to 900 nm, with a total of 185 image bands. The spectral resolution was thus 2.43 nm.

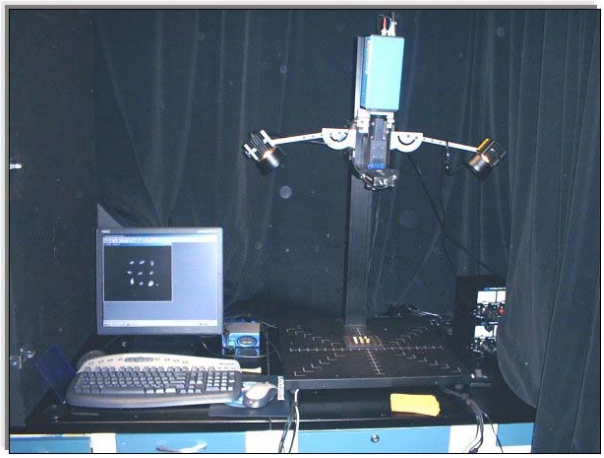

Figure 1. The VNIR-100E hyperspectral imaging system

Experiments

Experiment Design and Implementation

Five different toxin producing fungi were used in this study. The names and the toxins produced by each fungus are listed in Table 1. Among the five listed, were four different genera, and two from the same genus, but different species. All the fungi were obtained from the Food and Feed Safety laboratory, SRRC (Southern Regional Research Center), USDA (United Stated Department of Agriculture), New Orleans, LA. Subsequent fungal culture preparation and imaging was also conducted at the SRRC research Lab.

Table 1. Fungi and their toxic metabolites used in the experiment

Item	Name	Toxin producing	Toxin Name
1	*Penicillium chrysogenum*	Yes	Roquefortine C, chrysogine, and meleagrin
2	*Fusarium moniliforme*	Yes	Acetyl T-2 toxin, calonectrin, butenolide, fusaric acid, fusarin, and vomitoxin, etc.
3	*Aspergillus parasiticus*	Yes	Aflatoxin
4	*Trichoderma viride*	Yes	Trichodermin
5	*Aspergillus flavus*	Yes	Aflatoxin

The experiment had two parts, A and B. Fungi were cultured on plastic Petri-dishes/plates on potato dextrose agar (PDA) medium in an incubator at 30^{o}C. In Part A, each fungus was inoculated at the center of a single dish with 10 ul of the respective inoculum. In Part B, all five isolates were inoculated at different spots on the same dish with 5 ul of inoculum. (see figure 2 for fungi seeding sequence).

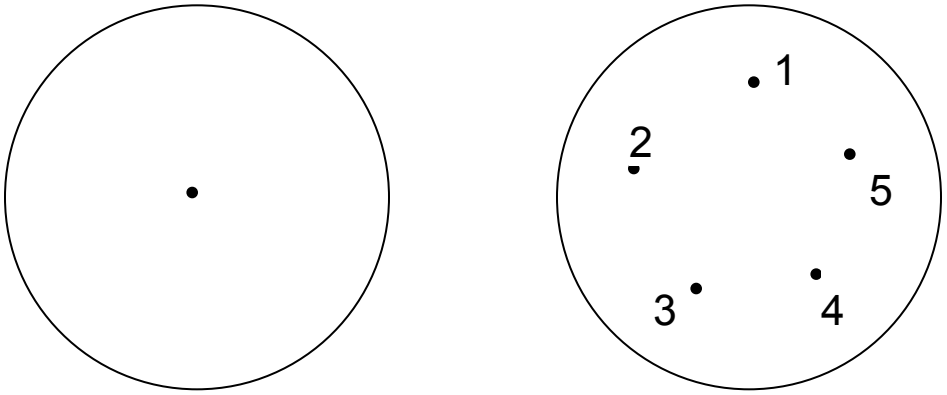

Figure 2. Fungal inoculation schema for both parts of the experiment. The black dots are the designated inoculation spots within the Petri-plate. The numbers in Part B represent the item numbers of different isolates. See Table 1 for the name of each isolate.

In Part A, each isolate had two replications resulting in a total of ten plates used in this part of the experiment. The experiment followed a complete randomized design. PDA medium was poured into all ten plates and cooled. For each isolate, two plates were randomly selected and 10 μl of inoculum was introduced to the center of each plate. Fungi were grown in a 30 ^{o}C incubator in the dark.

In Part B, there were five dishes used, representing five replications. In order to avoid crowding and growth overlap, 5 μl of inoculum from each isolate was introduced with a pipette to the designated spot for the corresponding isolate, respectively. Fungi were grown in the same manner as in Part A of the experiment.

Image Acquisition

Images for both experiments were taken on growth day 5 using experiment settings described previously. All dishes from each experiment were imaged in random order. After imaging, all dishes were appropriately discarded. For image calibration, a dark current image and a standard reflectance image were taken in each experiment before imaging the fungi. The dark image data were taken with the camera lens completely blocked and a white diffuse reflectance standard panel 10×10 in². (Spectralon: SRT-99-100 UV-VIS-NIR Diffuse Reflectance Target, LabSphere Inc.) was used to take the reference reflectance data.

Image Processing and Data Analysis

Hyperspectral Image Preprocess

A series of pre-processing steps were applied to each raw hyperspectral image, in the same manner as described previously in Yao et al. (2004). The imaging sensor recorded only raw digital counts of reflectance. Therefore, the dark and the reference images taken before each experiment were used to convert the raw digital counts to percent reflectance. For reflectance calibration, the following equation was used:

$$Reflectance_{\lambda} = \frac{S_{\lambda} - D_{\lambda}}{R_{\lambda} - D_{\lambda}} \times 100\% \qquad \text{Equation 1}$$

where Reflectance λ is the reflectance at wavelength λ; S_{λ} is the sample intensity at wavelength λ; D_{λ} is the dark intensity at wavelength λ; R_{λ} is the reference intensity at wavelength λ. After preprocessing, the calibrated image has185 bands with wavelength range from 450 nm to 900 nm. The image size is 688 × 525 pixels and the image size is 261 Mbyte.

Image Processing and Data Analysis

Experiment A:

Experiment A was intended for mold classification and pure fungal signature extraction. Experiment A used a single dish for culturing each individual fungal isolate in duplicate. The two replications of all five fungi were mosaiced together to form one large image. Next, a small area of growth region for each fungus was selected as training region of interest. The selection focused on a mature fungal culture. Similarly, validating data was also selected from the mosaic image.

Table 2. Selected training and validation pixels for experiment A.

Fungal class	Pixel Numbers				
	Fusarium	*A. flavus*	*Trichoderma*	*A. parasiticus*	*Penicillium*
Training	7248	*7135*	7597	*7858*	6674
Validation	79282	91130	198231	63322	10999

When applying image classification, different supervised classification algorithms were first tested. The algorithms tested were binary encoding, parallel piped, Spectral Angle Mapper, minimum distance, Mahalanobis Distance, Maximum Likelihood (ML), and binary encoding (ENVI, 2000). Based on the initial results, it was decided to use Maximum Likelihood for further investigation. The problem with Maximum Likelihood algorithm is that it took approximately 10 hours to complete the 5 Gbyte, 185 bands mosaic image on a 1 G hertz Pentium computer.

At this point, image dimension reduction was needed to speed up the classification process. A previous study (Hughes, 1968) indicated that classification accuracy could be improved for high dimension data such as hyperspectral image, by reducing dimensionality. The training data was extracted and processed in a SAS STEPDISC (SAS, 2003) procedure to obtain the most significant image bands. Based on the result of the STEPDISC procedure, the top 10 image bands were used in the ML classification. This time the classification time was reduced to 10 minutes. Classification accuracy was subsequently assessed at this point.

Once the classified image was obtained, the classified region for each fungus was used to extract pure fungal signature and to compute class statistics such mean and covariance. This information is useful as it could be assumed as standard classification training data and used for future classification and identification. In addition, pair-wise fungal class separability measurements were computed using the classified image. The separability measurements were computed as Jeffries-Matusita and Transformed Divergence.

Experiment B:

Experiment B is for mixed fungi classification using training data (pure fungal signatures) obtained from experiment A. Similar to experiment A, the five replicates of dishes, each with five cultured fungi, were mosaiced into a single image. The validation pixel number for each isolate is showed in Table 2. ML classification was run with the 10 most significant image bands identified in experiment A. Classification accuracy was also assessed accordingly.

Table 3. Selected validation pixels for experiment B. The training data was obtained from experiment A.

Fungal class	Pixel Numbers				
	Fusarium	*A. flavus*	*Trichoderma*	*A. parasiticus*	*Penicillium*
Validation	54835	72868	95888	65387	30047

Results and Discussions

Experiment A:

Figure 3 is the true color image for all fungal isolates in experiment A. The name sequence can be found in Table 4. Different isolates exhibit different growth pattern. For example, *Penicillium* took only a small fraction of the Petri dish. This indicates *Penicillium* does not grow aggressively over the 5-day culture period. On the other hand, *Trichoderma* displays a very aggressive growth as it expanded over the entire Petri dish. The other three fungi, *Fusarium*, *A. flavus*, and *A. parasiticus* showed moderate growth. *Fusarium* has a distinct white (with pink in the inoculation point) color compared to the other fungi. The two Aspergilli have similar growth patterns and slightly different color.

Table 4. Corresponding name for the above image

Penicillium chrysogenum	*Penicillium chrysogenum*	*Fusarium moniliforme*
Fusarium moniliforme	*Aspergillus parasiticus*	*Aspergillus parasiticus*
Trichoderma viride	*Trichoderma viride*	*Aspergillus flavus*
Aspergillus flavus	None	none

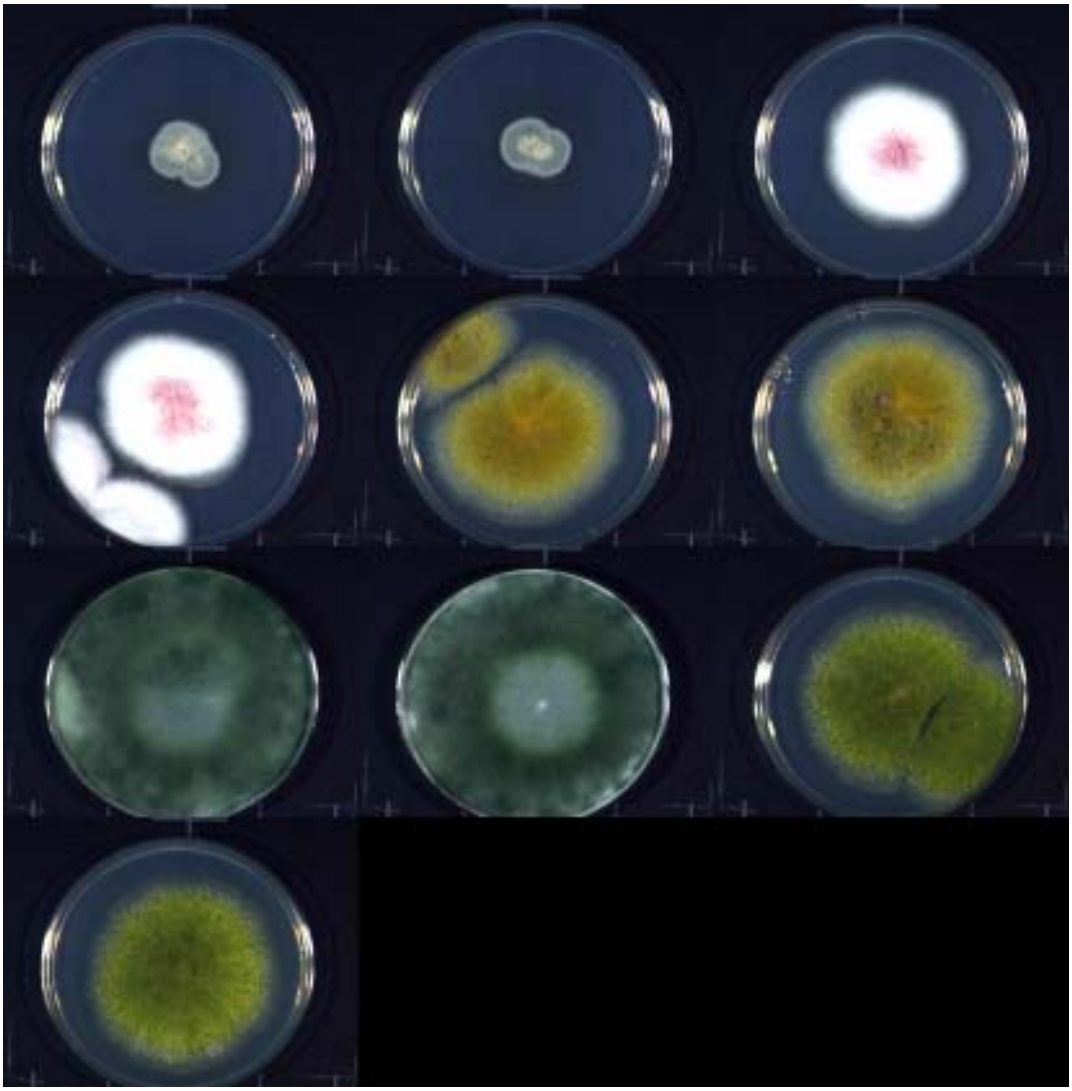

Figure 3. True color mosaic of the fungi used in experiment A.

When doing image classification, the initial ML classification with all 185 bands took a long time to process. A reduced image space is desired in order to reduce the amount of time for image classification. In addition, because neighboring hyperspectral images are highly correlated with each other, this correlation affects correct estimation of class statistics for a parametrical classifier such as ML, which may lead to decreased classification accuracy. A reduced image space, such as the stepwise discriminant analysis-ranked image bands used in this paper, would improve class statistics estimation, and consequently improve the overall classification accuracy. Table 2 presents the first10 image bands selected from stepwise discriminant analysis. For the 10 bands, three are in the blue region (450 nm, 458 nm, and 478 nm), three are in the green region (509 nm, 541 nm, 572 nm), two are in the red region (616 nm, 670 nm), and two are in the near infrared region (743 nm, 864 nm). All bands are significant with $p < 0.0001$.

Table 5. Results of SAS STEPWISE procedure for experiment A with statistics of the first 10 selected bands.

Step	Band	Wavelength (nm)	Partial R-square	F-Value	P-value	Wilks' Lambda	Pr < Lambda	Average Squared Canonical Correlation
1	B121	743	0.9754	405843	<.0001	0.024603	<.0001	0.162566
2	B4	458	0.8855	79194.9	<.0001	0.002816	<.0001	0.310004
3	B38	541	0.6996	23839.6	<.0001	0.000846	<.0001	0.397645
4	B69	616	0.5942	14990.6	<.0001	0.000343	<.0001	0.466925
5	B171	864	0.3755	6153.92	<.0001	0.000214	<.0001	0.482929
6	B13	478	0.3348	5150.82	<.0001	0.000143	<.0001	0.493671
7	B91	670	0.2051	2640.96	<.0001	0.000113	<.0001	0.501568
8	B1	450	0.1564	1897.59	<.0001	9.56E-05	<.0001	0.508803
9	B25	509	0.157	1906.26	<.0001	8.06E-05	<.0001	0.515065
10	B51	572	0.1552	1881.04	<.0001	6.81E-05	<.0001	0.518388

The classification accuracy results are presented in a confusion matrix expressed in Table 6. Both *Fusarium* and *Penicillium* have high classification accuracy. The numbers are 99.2% and 99.9%, respectively. These numbers indicate *Fusarium* and *Penicillium* can be readily identified from the 5 candidate molds. The next to best accuracy is for *Trichoderma*, which is 98.6%. Error rate for the two *Aspergilli* are higher than the other three molds. The accuracy readings are 95.2% and 96.4% for *A. flavus* and *A. parasiticus*, respectively. The ML classifier is somewhat confused in classifying the two *Aspergillus* species. About 4.6 % of *A. flavus* was classified as *A. parasiticus.* Conversely, 1.7% of *A. parasiticus* was classified as *A. flavus*. Another 1.7% of *A. parasiticus* was classified as *Penicillium*.

The overall classification accuracy for experiment A is 97.7%. One thing that the readers need to be aware is that the validation data set was selected manually, thus the result was to some extent subjective.

Table 6. Confusion matrix used in assessing classification accuracy of experiment A using the 10 most significant bands in Table 5. The overall accuracy is 97.7276% (432898/442964) with the Kappa Coefficient equals 0.9679.

Class	Ground Truth (Pixels)					
	Fusarium	*A. flavus*	*Trichoderma*	*A. parasiticus*	*Penicillium*	Total
Fusarium	78638	0	0	75	0	78713
A. flavus	0	86752	8	1094	0	87854
Trichoderma	0	40	195475	0	13	195528
A. parasiticus	0	4265	0	61047	0	65312
Penicillium	644	73	2748	1106	10986	15557
Total ground truth pixels	79282	91130	198231	63322	10999	442964

Figure 4 is a plot of the five fungal signatures extracted from the classified image in experiment A. Because each isolate was cultured in an individual dish and every effort was made to prevent cross contamination among the samples, the displayed fungal reflectance signature is assumed to be a pure signature. In experiment B, these signatures along with the calculated class statistics will be used as training data for further classification of fungi.

In Figure 4 it can be seen that the reflectance of *Fusarium* is quite different from the other four isolates. This agrees with the previous observation in Figure 3. Trichoderma and *Penicillium* have similar reflectance shapes, but different magnitudes. *A. flavus* and A. *parasiticus* reflectance is not separable in the blue region, but starts to separate from the middle of the green region. Both *Aspergillus* species show stronger reflectance in the near infrared region than the visible light region, which is similar to reflectance measured over the canopy of a typical plant.

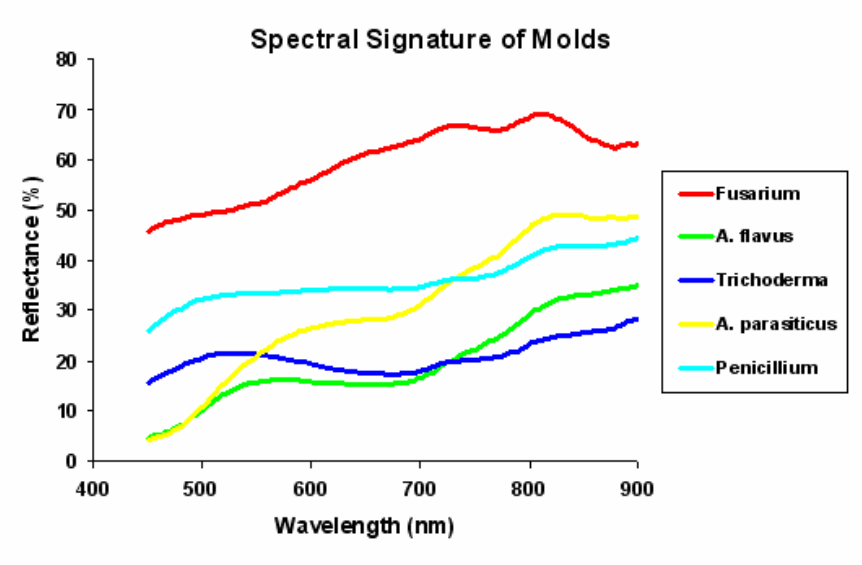

Figure 4. Mold spectral curves

Both the Jeffries-Matusita and Transformed Divergence (Richard and Jia, 1999) are calculated and presented in Table 6 as fungal class separability measurements. The input classes of fungi were based on the ML classified image. Generally, these values should range from 0 to 2.0 and indicate how well the selected class pairs are statistically separable. Values greater than 1.9 indicate that the class pairs have good separability. It can be concluded that the classes are well separable based on fungal spectral reflectance.

Table 6. Separability measurements of the fungal classes – Jefferies Matusita

Jefferies_Matusita	*Fusarium*	*A. flavus*	*Trichoderma*	*A. parasiticus*	*Penicillium*
Fusarium		2.000	2.000	2.000	2.000
A. flavus	2.000		2.000	1.990	2.000
Trichoderma	2.000	2.000		2.000	2.000
A. parasiticus	2.000	1.990	2.000		2.000
Penicillium	2.000	2.000	2.000	2.000	

Table 7. Separability measurements of the fungal classes – Transformed Divergence.

Transformed Divergence	*Fusarium*	*A. flavus*	*Trichoderma*	*A. parasiticus*	*Penicillium*
Fusarium		2.000	2.000	2.000	2.000
A. flavus	2.000		2.000	1.996	2.000
Trichoderma	2.000	2.000		2.000	2.000
A. parasiticus	2.000	1.996	2.000		2.000
Penicillium	2.000	2.000	2.000	2.000	

Experiment B.

Figure 5 is the true color image for all fungal isolates in experiment A. The name sequence can be found in Figure 2. The growth pattern is similar to experiment A. One phenomenon seen in experiment A is the rapid expansion of *Trichoderma*, which overtook the entire Petri dish during the culture period. This same phenomenon can also be seen in experiment B. While the other four isolates all had moderate growth regions, *Trichoderma* spread out from the lower-right corner and "invaded" regions used by other isolates. One consequence is that the other four isolates might be contaminated by *Trichoderma*, which in turn will make fungal classification much more difficult in experiment B than in experiment A.

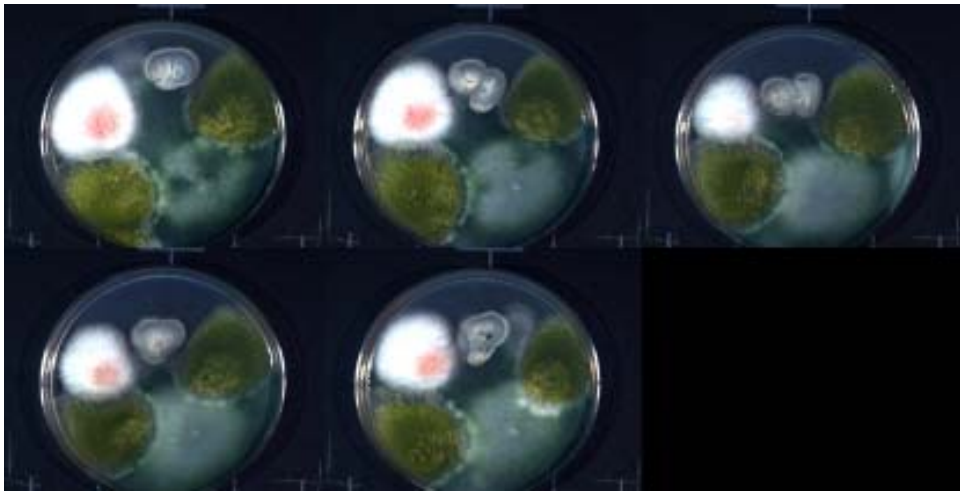

Figure 5. True color mosaic of the fungi used in experiment B.

The classification accuracy results for experiment B are presented in a confusion matrix expressed in Table 6. The overall classification accuracy value for experiment A is 71.53%. For individual fungi, the accuracy is 99.6%, 97.1%, 70.6%, 8.3%, and 98.4% for *Fusarium, A. flavus*, *Trichoderma, A. parasiticus*, and *Penicillium*, respectively. The largest drop of classification accuracy is for *A. parasiticus*. One reason is the contamination caused by *Trichoderma*, which is located next to *A. parasiticus*. Interestingly, contamination from *Trichoderma* did not have a strong influence over *A. flavus.* The effect is probably due to difference in growth rates between the isolates. Classification accuracy for *Fusarium* and *Penicillium* remains equivalent to experiment A.

Table 6. Confusion matrix used in assessing classification accuracy of experiment B using the 10 most significant bands in Table 5. The overall accuracy is 71.53%, with the Kappa Coefficient equals 0.6398.

Class	Ground Truth (Pixels)					
	Fusarium	*A. flavus*	*Trichoderma*	*A. parasiticus*	*Penicillium*	Total
Fusarium	54648	0	0	1	59	54708
A. flavus	0	70801	61	59955	48	130865
Trichoderma	0	139	67745	1	346	68231
A. parasiticus	0	1921	621	5420	23	7985
Penicillium	187	7	27461	10	29571	57236
Total ground truth pixels	54835	72868	95888	65387	30047	319025

Conclusion

This paper studied reflectance of five toxigenic fungi including *Fusarium*, *A. flavus*, *Trichoderma, A. parasiticus*, and *Penicillium* using visible near infrared hyperspectral imagery collected with a pushbroom image sensor. There were two experiments in this study. In experiment A, each fungus was cultured in individual Petri dish. In experiment B, all five species were cultured in a single dish. Images were classified in a reduced image space with 10 bands selected from the original images. The overall fungal classification accuracy in experiment A is 97.7% while in experiment B the accuracy dropped to 71.5%. The reason is because the fast growing of Trichoderma in experiment B contaminated spectral reflectance features of other isolates. Separability analysis of the pure fungal signatures in experiment A indicates the five fungi are separable to a high degree of accuracy.

Acknowledgements

Funding for the current project was provided through the USDA Specific Cooperative Agreement No. 58-6435-3-0121.

References

Aja-Nwachukwu, J. and S. O. Emejuaiwe. 1997. Alfatoxin-producing fungi associated with Nigerian maize. *Environmental Toxicology and Water Quality: An International Journal* 9:17-23

Aziz, N. H. and A. A. M. Shahin. 1997. Influence of other fungi on aflatoxin production by Aspergillus Flavus in Maize Kernels. *Journal of Food Production* 17: 113-123

Birth, G. S. and R. M. Johnson. 1970. Detection of mold contamination in corn by optical measurement. *J. Assoc. Off. Anal. Chem*. 53(5): 931-936

Brown, R. L., Z. Y. Chen, A. Menkir, T. E. Cleveland, K. Cardwell, J. Kling and D. G. White. 2001. Resistance to aflatoxin accumulation in kernels of maize inbreds selected for ear rot resistance in West and Central Africa. *J Food Prot.* 64(3): 396-400.

Dutta, T. K. and P. Das. 2001. Isolation of aflatoxigenic strains of Aspergillus and detection of aflatoxin B1 from feeds in India. *Mycopathologia* 151(1): 29-33.

ENVI, 2000. *ENVI Users Manual*. Boulder, CO: Research Systems, Inc.

Fente, C. A., J. J. Ordaz, B. I. Vazquez, C. M Franco, and A. Cepeda. 2001. New additive for culture media for rapid identification of aflatoxin-producing Aspergillus strains. *Applied and Environmental Microbiology* 67(10): 4858-4862

Gordon, S. H., R. B. Schudy, B. C. Wheeler, D. T. Wicklow, and R. V. Greene. 1997. Identification of Fourier transform infrared photoacoustic spectral features for detection of Aspergillus flavus infection in corn. *International Journal of Food Microbiology* 35(2):179-186

Gordon, S. H., B. C. Wheeler, R. B. Schudy, D. T. Wicklow, and R. V. Greene. 1998. Neural Network pattern recognition of photoacoustic FTIR spectra and knowledge-based techniques for detection of mycotoxigenic fungi in food grains. *Journal of Food Protection* 61(2):221-230

Gordon. S. H., R. W. Jones, J. F. McClelland, D. T. Wicklow, and R. V. Greene. 1999. Transient infrared spectroscopy for detection of toxigenic fungi in corn: potential for on-line evaluation. *Journal of Agricultural and Food Chemistry* 47: 5267-5272

Greene. R. V., S. H. Gordon, M. A. Jackson, G. A. Bennett, J. F. McClelland, and R. W. Jones. 1992. Detection of Fungal Contamination in corn: Potential of FTIR-PAS and –DRS. *Journal of Agricultural and Food Chemistry* 40:1144-1149

Hughes, G. F. 1968. On the mean accuracy of statistical pattern recognition. *IEEE Transactions on Information Theory* 14:55 – 63.

Kim, I., M. S. Kim, Y. R. Chen, and S. G. Kong. 2004. Detection of skin tumors on chicken carcasses using hyperspectral fluorescence imaging. *Transactions of the ASAE* 47(5): 1785-1792

Lawrence, K. C., B. Park, W. R. Windham, C. Mao. 2001. Calibration of imaging spectrometry system for inspection of contaminated poultry carcasses. ASAE Paper No. 013129. St. Joseph, Mich.: ASAE.Lu, R. 2003. Detection of bruises on apples using near–infrared Hyperspectral imaging. *Transactions of the ASAE* 46(2): 523–530.

Malone, B. R., C. W. Humphrey, T. R. Romer and J. L. Richard. 2000. Determination of aflatoxins in grains and raw peanuts by a rapid procedure with fluorometric analysis. *J AOAC Int*. 83(1): 95-8.

Richards, J. A. and X. Jia. 1999. *Remote Sensing Digital Image Analysis*, Springer-Verlag, Berlin, p. 240.

SAS. 2003. *SAS Users Manual*. Cary, N.C.: SAS Institute, Inc.

Yabe, K., Y. Ando, M, Ito, and N. Terakado. 1987. Simple method for screening aflatoxin-producing molds by UV photography. *Appl Environ Microbiol* 53(2):230-4

Yao, H., Z. Hruska, K. DiCrispino, D. Lewis, J. Beach, R. L. Brown, and T. E. Cleveland. 2004. Hyperspectral Imagery for Characterization of Different Corn Genotypes. *Proc. of SPIE, Optic East, a SPIE Conference on Nondestructive sensing for food safety, quality, and natural resources.*

Zachova, I., J. Vytrasova, M. Pejchalova, L. Cervenka and G. Tavcar-Kalcher. 2003. Detection of aflatoxigenic fungi in feeds using the PCR method. *Folia Microbiol* (Praha) 48(6): 817-21.

Zeringue, H. J. Jr., B. Y. Shih, K. Maskos and D. Grimm. 1999. Identification of the bright-greenish-yellow-fluorescence (BGY-F) compound on cotton lint associated with aflatoxin contamination in cottonseed. *Phytochemistry* 52(8): 1391-7.